SAND2019-9772D

Can water-rich melts in the Earth's upper mantle be seismically detected? A shockless-compression study on Thor.

Lindsay M. Harrison[1], Alisha N. Clark[1], Steven D. Jacobsen[2], Adam R. Sarafian[3], Jean-Paul Davis[4], Brian S. Stoltzfus[4], J. Matthew Lane[4], Kyle R. Cochrane[4], Joshua P. Townsend[4], and Christopher T. Seagle[4]

[1] University of Colorado Boulder, Department of Geological Sciences; [2] Northwestern University, Department of Earth and Planetary Sciences; [3] Corning Inc.; [4] Sandia National Laboratories

I. Motivation

The earth's mantle transition zone (MTZ) is defined as the region between seismic discontinuities at 410-km (12 GPa) and 660-km (28 GPa) depths. Low seismic velocities observed just above and just below the MTZ are commonly attributed to the presence of partial melts (Schmandt et al. 2014; Song et al. 2004). But present-day geotherm is **below** solidus of mantle minerals. Polymorphs of $MgSiO_4$, the major mantle phase, inside MTZ have high water solubility, while those above and below do not. If MTZ hydrated, then mantle convection can cause melt at the upper and lower boundaries of the MTZ by dehydration reactions. Evidence has been growing that the mantle transition zone (MTZ) contains a significant amount of water predominantly in the recent discoveries of water in deep-mantle diamond inclusions (e.g. Pearson et al. 2014). Thus, there is an increased interest in equation-of-state (EOS) measurements of silicate melts & glasses at MTZ pressures.

In order to interpret seismic velocities at the MTZ and constrain the volatile content of melts, we need to understand the effect of volatiles on the velocities of silicate melts at high pressure. We will be performing ramp compression experiments on hydrous and anhydrous amorphous silicates on Thor. Ramp compression on Thor is isentropic and so will more closely mimic earth's current thermal state than shock compression. We will be capable of measuring the sound velocity and density of hydrous and anhydrous melts at pressures through 30+ GPa spanning pressure relevant to the generation of hydrous melt in the present-day deep Earth.

This work is being performed as complementing development experiments to characterize sample materials in support of Z-Machine Fundamental Science Project "*Origin of Earth's water: Role of hydrous melts at extreme P-T conditions*". This project is currently ongoing with a Z-shot scheduled this Fall to shock-melt then ramp hydrous silicate glasses.

II. Geologic background

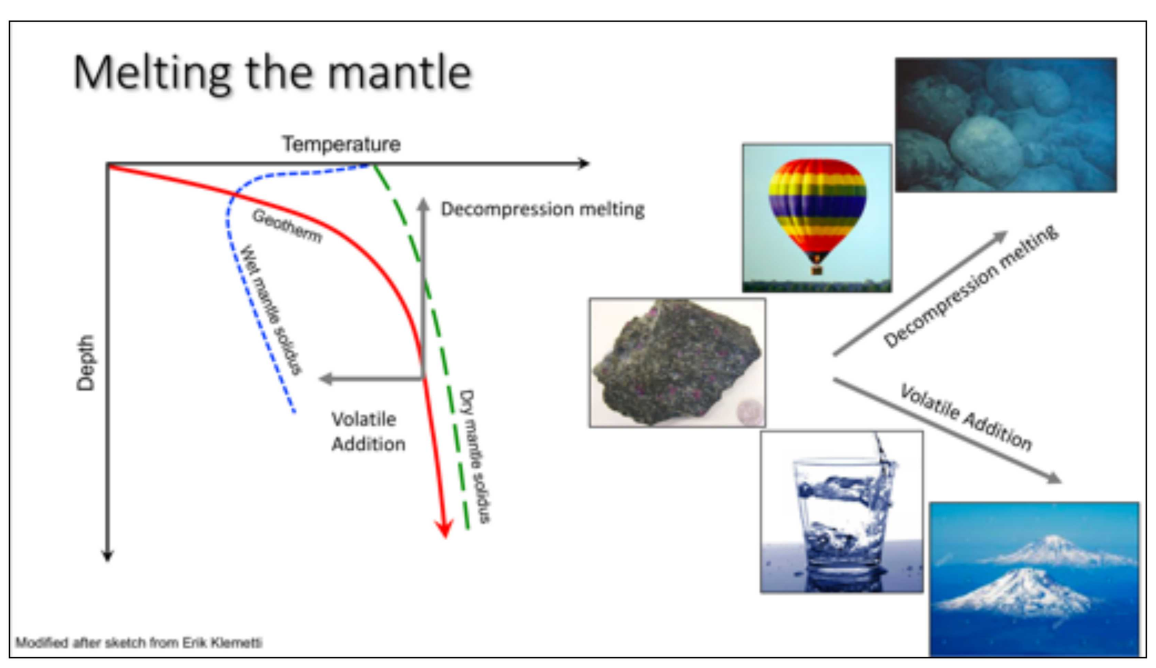

Fig. 1: Regions in the Earth that have lower seismic velocity than the global average are often attributed to the presences of silicate melts and/or volatile-rich fluids. Melt can be generated by decompression melting and melting point depression, which can occur with addition of volatiles.

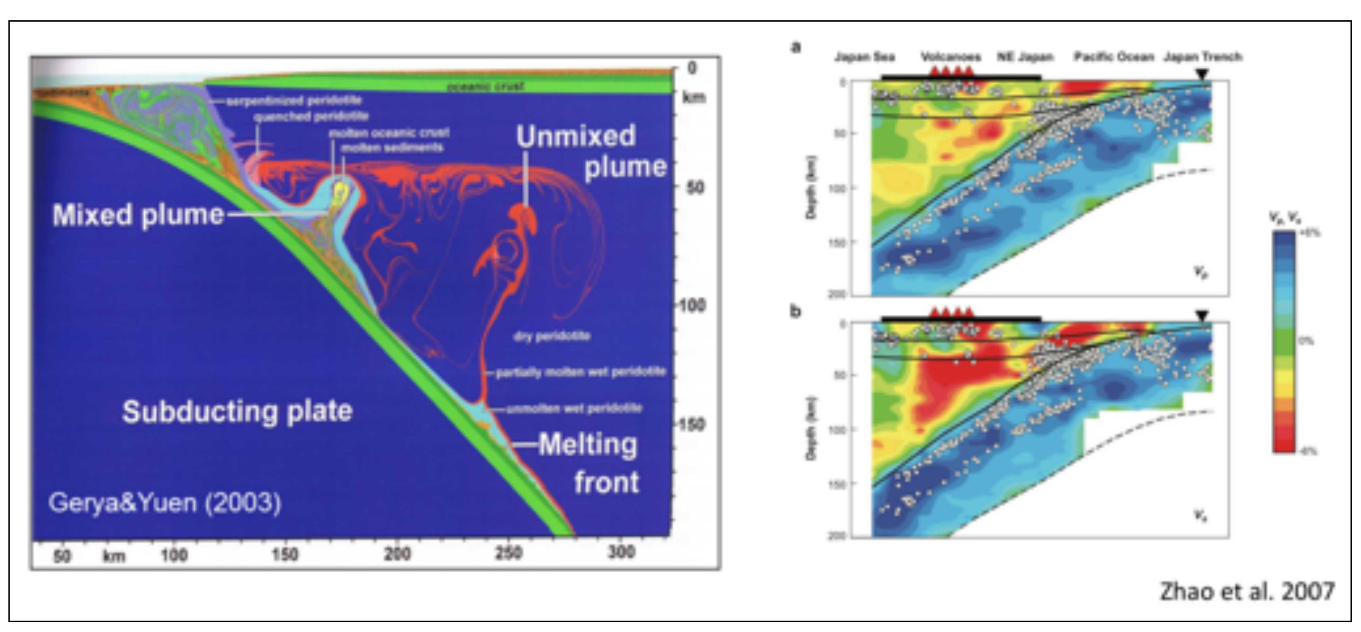

Fig. 2: Two regions where we think that volatile addition plays an important role in the production of melt (and the observation of low seismic velocities) are 1) in subduction zones (arc volcanism, which can be sampled directly from erupted magmas) and 2) above and below the mantle transition zone (samples by deep diamond inclusions).

II. Volatiles in silicates

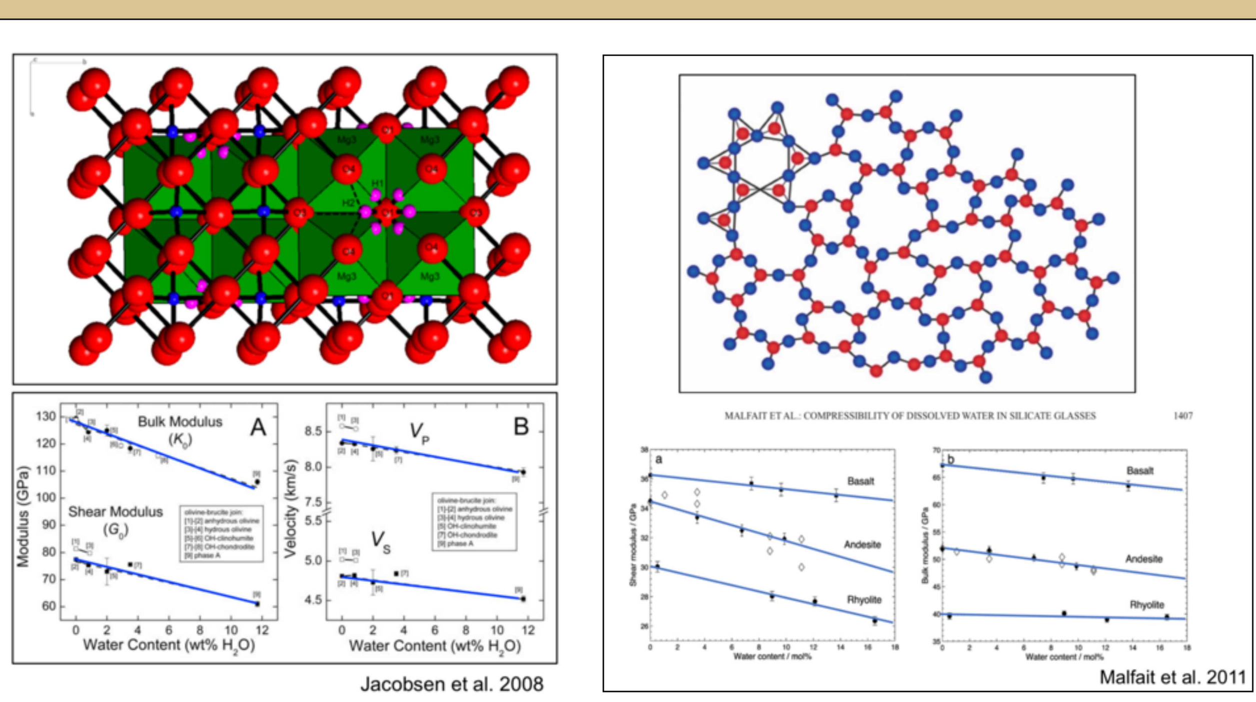

Fig. 3: Crystalline silicates (left) - water is stored as hydroxyl (OH) units and charge balanced by defects (vacancies). This leads to slower velocities and softer elastic moduli with increasing water content. A similar effect is observed at one atmosphere for amorphous silicates (right).

III. Compression of volatile-rich silicate glasses

On compression, volatile-rich silicate glasses are stiffer than their anhydrous counterparts.

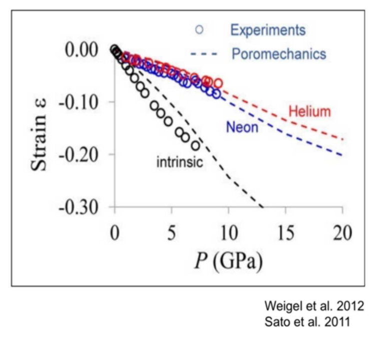

Fig. 4: SiO_2 glass is stiffer when saturated with noble gases.

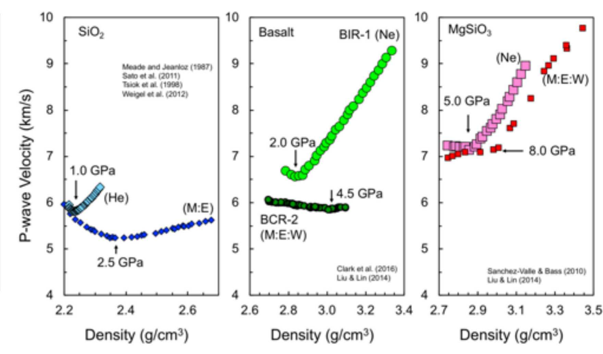

Fig. 5: Acoustic velocities are faster in the presence of noble gases for SiO_2, basalt, and $MgSiO_3$ glasses.

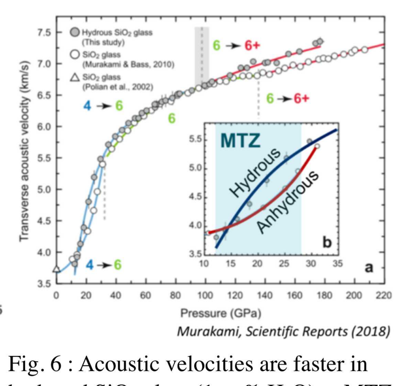

Fig. 6: Acoustic velocities are faster in hydrated SiO_2 glass (1 wt% H_2O) at MTZ pressures than anhydrous SiO_2 glass.

IV. Mechanisms of volatile incorporation & densification

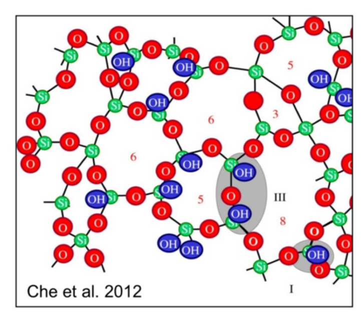

Fig. 7: Formation of silanol groups.

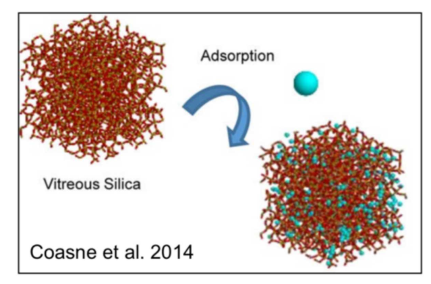

Fig. 8: Filling of interstitial void space.

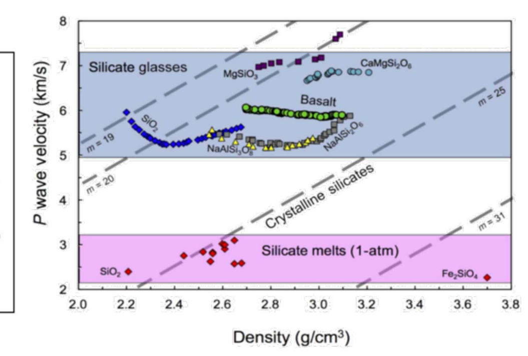

Fig. 9: Densification shows anomalous compressibility where the acoustic velocity depends weakly on pressure and density.

V. Summary

H_2O incorporated differently in amorphous silicates than into crystalline materials

- Fill interstitial voids and/or bond as silanol (Si-O-H) group
- Reduces compressibility (stiffer compression response)
- Effect's dependence on pressure, temperature, composition unknown
- Hydration-dependence of elastic properties under quasi-isentropic (ramped) compression needed to interpret MTZ-related seismic data

VI. Methods

The Thor64 pulsed-power machine is a new facility at Sandia for magnetically-driven dynamic shockless compression of materials

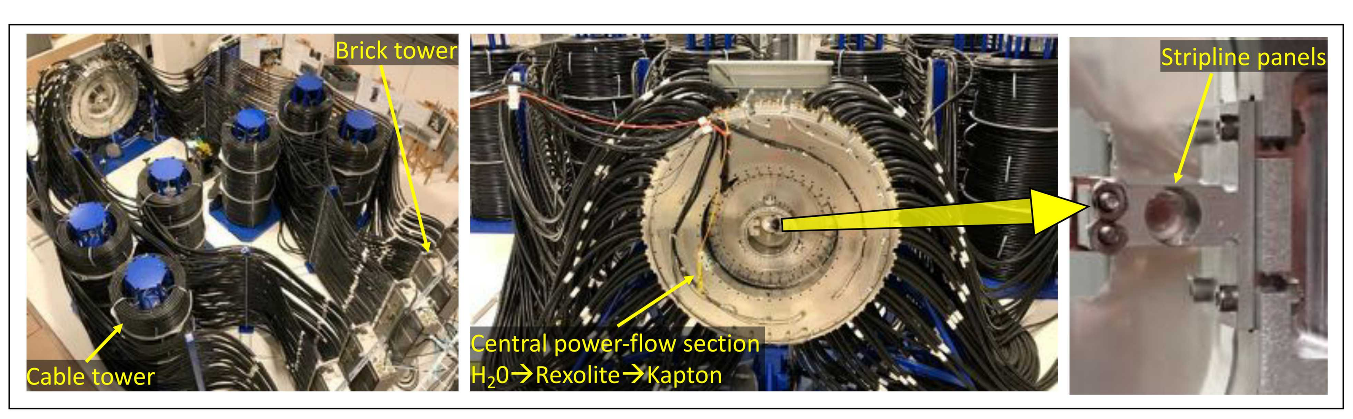

Fig. 10: Photographs of Thor. In the center photograph, the large round section is about 1.5 m in diameter.

- 64 "bricks" (2 capacitors + 1 switch) arranged in 8 towers
- Machine stores 51 kJ electrical energy when charged to 90 kV
- Switching all bricks synchronously delivers ~2.5 MA to a standard load
- Stripline = parallel flat-plate electrodes shorted at one end
- Ramped ***J***×***B*** force induces ramped stress wave in electrode material
- Wave propagates to sample material, de-coupled from magnetic field
- Both electrodes loaded identically while symmetric
- Fiber-coupled, laser-based velocimetry (PDV, VISAR)

Shockless compression is generated by ramp loading the sample (green boxes). Unlike a traditional shock experiment, pressure is generated solely from the magnetic field. There is not a flyer plate impact on the sample.

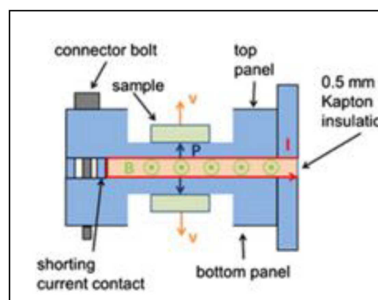

Fig. 11: (Above) Stripline panel geometry. I (red) is electrical current. B (green) is the magnetic field generated when the current shorts. P (black) pressure, and v (orange) is particle velocity.

Fig. 12: (Right) A close-up illustration of the sample. One side of the stripline measures the drive (LiF window only) while the other side has the LiF window glued on top of the silicate glass sample.

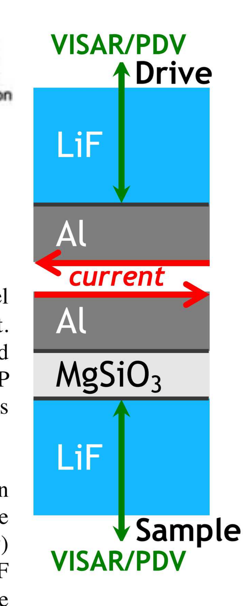

Thor64's modular energy storage and transit-time isolation allow simple yet fine control of the current pulse shape

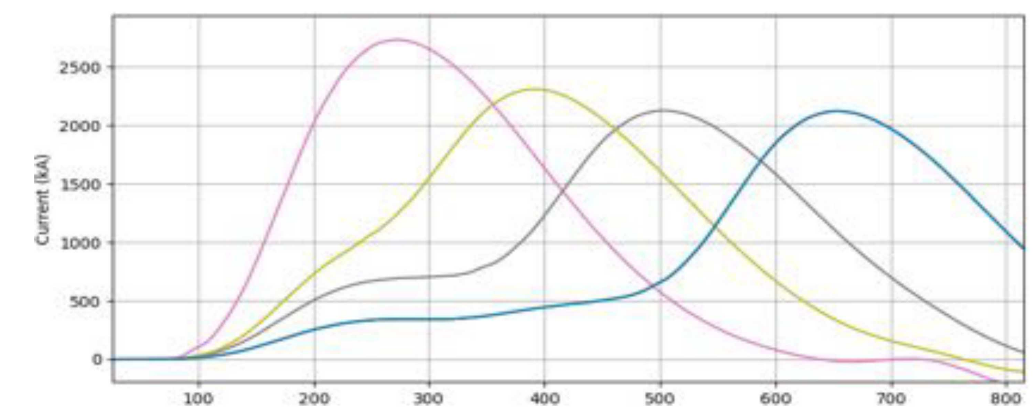

Fig. 13: A range of different pulse shapes. When all bricks are fired at once, the pink curve is produced (maximum current for Thor-64). When they are fired sequentially the timing and amplitude of the pulse shape can vary.

- Each brick can be independently switched (in practice, trigger them in groups of 4)
- Long cables → time isolation of switches
- 500-ns round-trip from brick to load and back = maximum spread in trigger times
- Vary loading rate by a factor of ~10 by changing trigger times and load panel width
- Increasing rise time decreases peak current → lower magnetic pressure for given load geometry
- Decreasing stripline panel width increases magnetic pressure → higher dP/dt for given pulse shape
- For shorter pulses ~2.4 MA peak current…
- 10-mm wide stripline → ~20 GPa
- 8-mm wide stripline → ~30 GPa
- 6-mm wide stripline → ~40 GPa
- Double-ramp pulse shapes, flat-topped pulse shapes, etc.

VII. Data processing

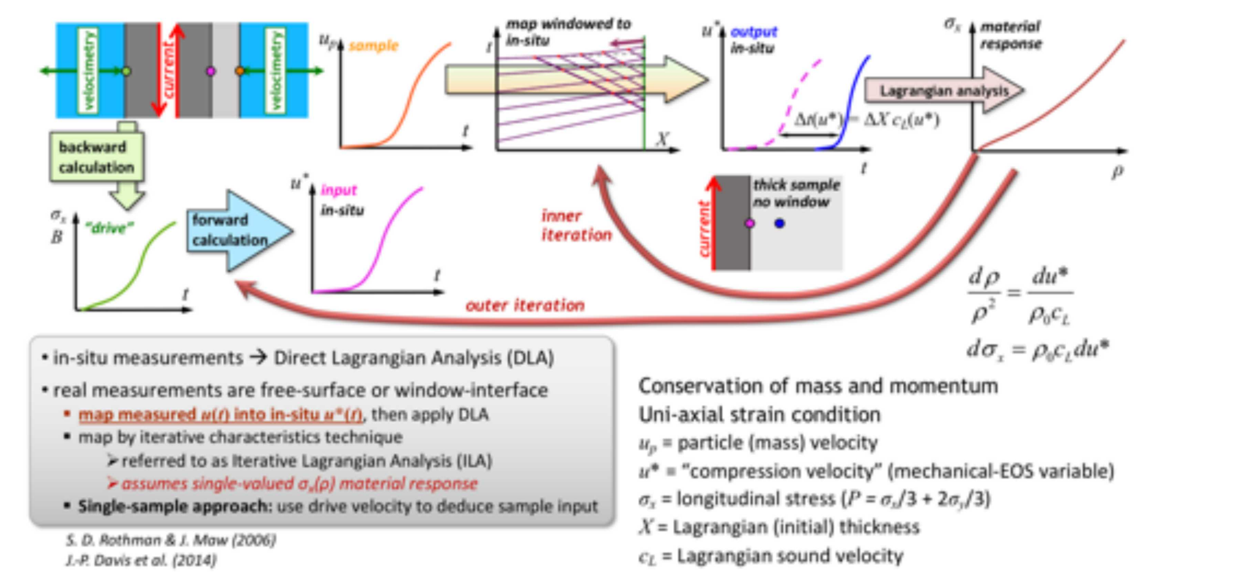

Fig. 14: Iterative Lagrangian analysis (ILA) determines stress-density path from velocimetry of LiF-windowed "drive" and sample. *S. D. Rothman & J. Maw (2006); J.-P. Davis et al. (2014)*

VIII. Preliminary results

Collaborating with Corning, Inc. to manufacture samples of hydrated silicate glasses

- Proprietary process based on pioneering work of R. F. Bartholomew et al. from 1980's
- Working on Mg-SiO_2, Na-SiO_2, and pure SiO_2 glasses with up to several weight-% water
- Samples available thus far for Thor experiments have been low-water $MgSiO_2$ (100/400 ppm) and SiO_2 (<0.5ppm/1000 ppm)

Six shots completed to date on Thor for MgSiO3 glass:

- HSG01 – dry, 440 μm, 10-mm wide panel
  Long shaped pulse (avoid shock)
- HSG02 – dry, 693 μm
  Smoother pulse shape
- HSG03 – dry, 455 μm
  Shorter pulse, higher P
- HSG04 – damp, 444 μm
  Repeat last pulse
- HSG05 – dry, 465 μm
  8-mm panel, higher P
- HSG06 – damp, 446 μm
  Repeat last pulse

- Diagnostics: PDV 4 channels and VISAR 8 channels

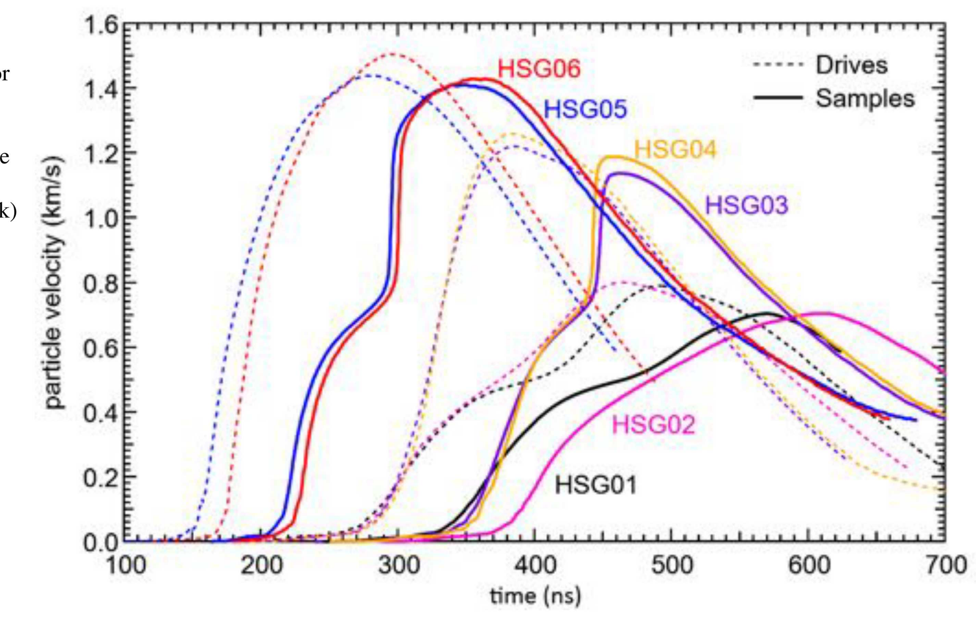

Fig. 15: Pulse shape for the drive (dashed) and sample response for six completed shots on Thor.

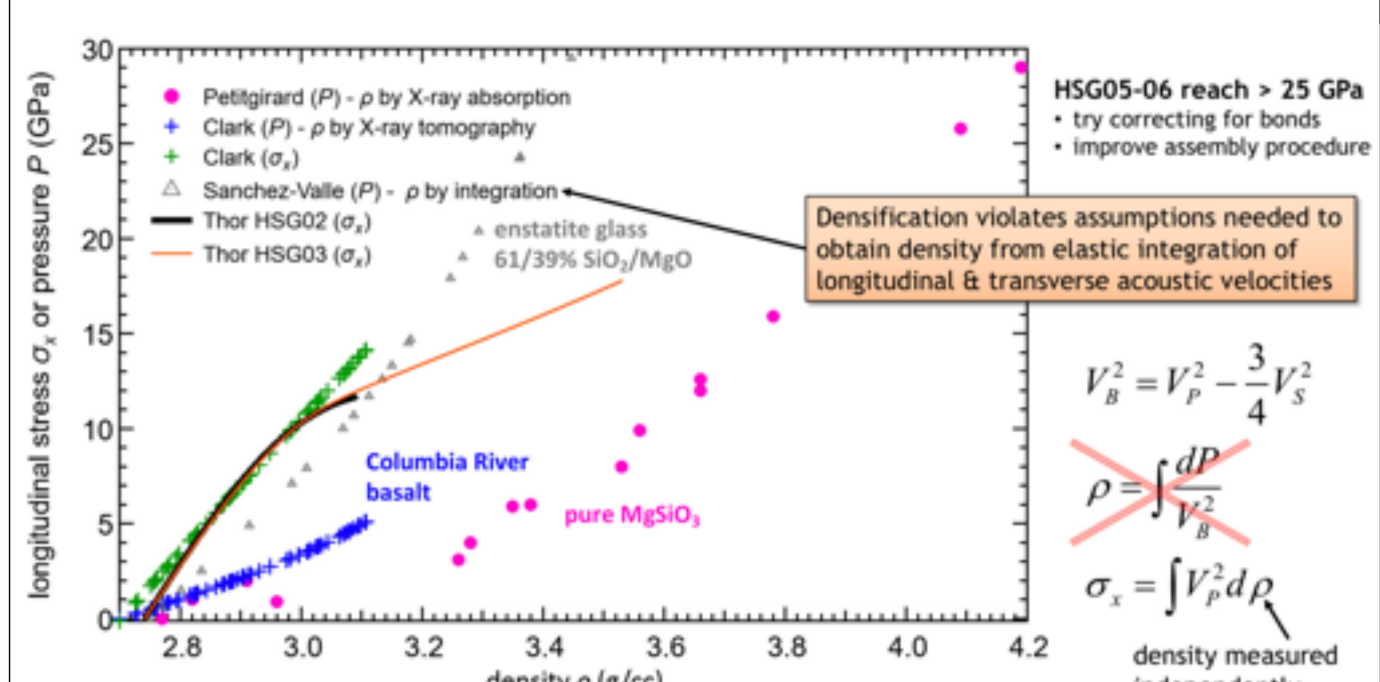

Fig. 16: Preliminary results of two Thor shots suggest densification begins above longitudinal stress of 10 GPa, not complete by 18 GPa.

XI. Next steps

1. Complete move to CU Boulder (Clark) and officially start grad school (Harrison)
2. Continue data analysis for MgSiO3 glasses (March-May 2019) and for SiO2 glasses (July 2019)
3. Further experiments as sample materials are prepared by Corning Inc.
4. Work with theory team of Cochrane, Townsend, and Lane for equation of state data that can will guide the shock-melt-then-ramp experiments for ZFSP shot on dry and hydrated SiO2 glasses to understand how volatiles are retained in melts during planetary impacts to determine the "*Origin of Earth's Water*."

We expect that the results of work will have significant impacts to both Earth/planetary and materials sciences.

References

Bercovici, D., & Karato, S. (2003). Whole-mantle convection and the transition-zone water filter. *Nature*, *425*(6953), 39–44.

Che, M., Mori, K., & Yamashita, H. (2012). Elaboration, characterization and properties of silica-based single-site heterogeneous photocatalysts. *Proceedings of the Royal Society A: Mathematical, Physical and Engineering Sciences*.

Clark, A. N., Lesher, C. E., Jacobsen, S. D., & Wang, Y. (2016). Anomalous density and elastic properties of basalt at high pressure: Reevaluating of the effect of melt fraction on seismic velocity in the Earth's crust and upper mantle. *Journal of Geophysical Research: Solid Earth*.

Clark, A. N., & Lesher, C. E. (2017). Elastic properties of silicate melts: Implications for low velocity zones at the lithosphere-asthenosphere boundary. *Science Advances*, *3*(12).

Davis, J.-P . et al. (2014). Analysis of shockless dynamic compression data on solids to multi-megabar pressures: Application to tantalum. *Journal of Applied Physics*.

Hirschmann, M. M. (2006). Water, melting, and the deep Earth H2O cycle. *Annu. Rev. Earth Planet. Sci*.

Jacobsen, S. D., et al. (2008). Effects of hydration on the elastic properties of olivine. *Geophysical Research Letters*.

Liu, J., & Lin, J.-F. (2014). Abnormal acoustic wave velocities in basaltic and (Fe,Al)-bearing silicate glasses at high pressures. *Geophysical Research Letters*.

Malfait, W. J., Sanchez-Valle, C., Ardia, P., Médard, E., & Lerch, P. (2011). Compositional dependent compressibility of dissolved water in silicate glasses. *American Mineralogist*.

Meade, C., & Jeanloz, R. (1987). Frequency-dependent equation of state of fused-silica to 10 GPa. *Physical Review B*.

Murakami, M. (2018). Water makes glass elastically stiffer under high-pressure. *Scientific Reports*.

Pearson, D.G. et al. (2014). Hydrous mantle transition zone indicated by ringwoodite included within diamond. *Nature*.

Petitgirard, S., et al. (2015). Fate of MgSiO3 melts at core–mantle boundary conditions. *Proceedings of the National Academy of Sciences*.

Sakamaki, T., et al. (2013). Ponded melt at the boundary between the lithosphere and asthenosphere. *Nature Geoscience*.

Sanchez-Valle, C., & Bass, J. D. (2010). Elasticity and pressure-induced structural changes in vitreous MgSiO3-enstatite to lower mantle pressures. *Earth and Planetary Science Letters*.

Sato, T., Funamori, N., & Yagi, T. (2011). Helium penetrates into silica glass and reduces its compressibility. *Nature Communications*.

Schmandt, B. Et al (2014). Dehydration melting at the top of the lower mantle. *Science*.

Song, T. R. A. et al.. (2004). Low-velocity zone atop the 410-km seismic discontinuity in the northwestern United States. *Nature*.

Tsiok, O. B. et al. (1998). Logarithmic kinetics of the amorphous-amorphous transformations in SiO2 and GeO2 glasses under high-pressure. *Physical Review Letters*.

Weigel, C. et al. (2012). Vitreous Silica Distends in Helium Gas: Acoustic Versus Static Compressibilities. *Physical Review Letter*).

Zhao, D. et al. (2007). Tomographic Imaging outside a Seismic Network : Application to the Northeast Japan Arc. *Bulletin of the Seismological Society of America*.

Acknowledgments

This work would not be possible without the collaboration made possible by generous support of the Z Fundamental Science Program. Our collaboration with Corning Inc. is instrumental in sample synthesis as well as scientific development. We wish to thank the DICE staff who have performed these experiments. A. N. Clark has been supported by NSF grant 1625205. Travel for L. Harrison to attend the ZFSP 2019 workshop has been made possible by NNSA Academic Programs and administered by Oak Ridge Institute for Science and Education.

Sandia National Laboratories is a multimission laboratory managed and operated by National Technology & Engineering Solutions of Sandia, LLC, a wholly owned subsidiary of Honeywell International Inc., for the U.S. Department of Energy's National Nuclear Security Administration under contract DE-NA0003525.